fibrotic tissue layer was observed surrounding the biorubber (**Figure 20 A–D**) and some host cells appeared to have migrated into the scaffold (**Figure 20 E** and **F**), no signs of immune response based on lymphocytic infiltration or giant body cells were detected.

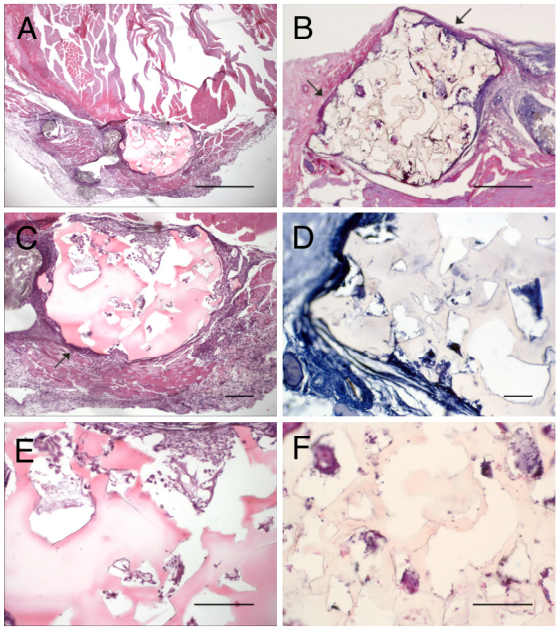

Figure 20: Histology of balb/c mice implants.
Tissue sections (10 μm) from IM implants at 15 days (**A, C, E**) or 45 days (**B, D, F**) post-implantation, stained with hematoxylin–eosin (**A–C**, **E, F**) or stained for biotin and counterstained with hematoxylin (**D**). RAD16-Ib was not detected while biorubber (star in **C, D**) was present in all sections of RAD16-I/biorubber implants. Arrow heads (**B, C**) point to the fibrotic layer surrounding biorubber scaffolds. Bars: **A, B** = 500 μm; **C, D, E, F** = 100 μm.

As was the case for normal mice, macroscopic evaluation of the implants from immunodeficient BALB/c nu/nu mice also failed to show signs of rejection or inflammatory reactions (**Figure 21 H, I, K, L**) and only the biorubber, but no RAD16-I, was detected at the IM and SC implantation sites. In this case, a layer of fibrotic tissue surrounding the implants was also detected.

4.2.7. Fluorescence analysis of implants from BALB/c nu/nu mice

Selected sections from nude mice IM implants of RAD16-I hydrogels and RAD16-I/biorubber composites seeded with G·Luc-C57BL/6 cells were deparaffined and stained by the Masson trichrome method, to reduce the muscle autofluorescence, and examined by fluorescence emission microscopy to determine the contribution of G·Luc-C57BL/6 cells. Images (**Figure 21 A–F, G, J**) showed that implants generating high BLI signals also contained more G·Luc-C57BL/6 cell clusters and total cells than implants producing lower BLI signals. Occasionally, IM implants showing no BLI signal had also some G·Luc-C57BL/6 cells. Thus, there was a strong correlation between the number of cells in the implants and the amount of light produced. However, no quantification was possible due to the difficulty of estimating fluorescent cell numbers in cell clusters.

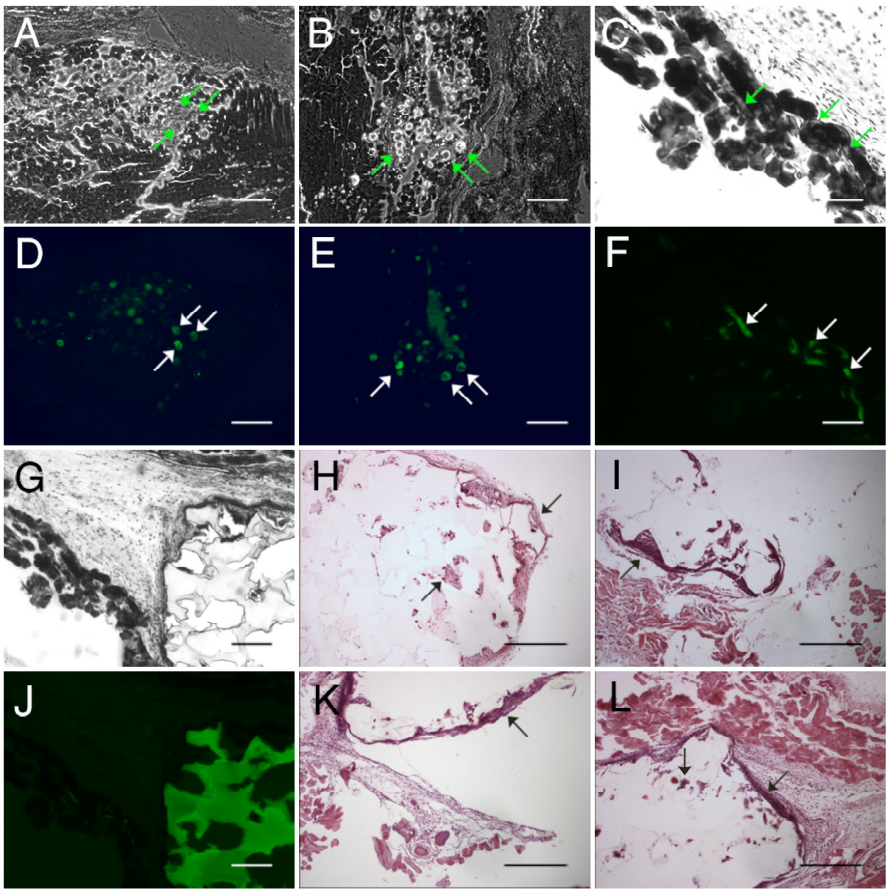

Figure 21: Histology of BALB/c nu/nu mice implants.
10 μm sections from RAD16-I (**A, B, D** and **E**) and RAD16-I/biorubber (**C, F, G–L**) composites seeded with G·Luc-C57BL/6 cells and implanted IM in nude mice during a 90-day period, showing high BLI signal. White light (**A–C, G**) and fluorescence microscope images using the GFP channel (**D–F, J**) of Masson's trichrome stained sections. G·Luc-C57BL/6 cell detection at the IM implantation sites (white and green arrows in **A–F**) was higher in seeded RAD16-I implantations than in seeded RAD16-I/biorubber implantations. (**J**) Biorubber showed high autofluorescence when visualized using the GFP microscope channel. (**H, I, K, L**) Hematoxylin–eosin stained sections showed biorubber maintenance after 90 days, from mice implanted with RAD16-I/biorubber scaffolds, and presence of fibrous tissue surrounding the implants (arrows). Bars = 200 μm.

4.2.8. Cell migration

Measurement of luciferase activity in brain, liver, spleen, lungs, bone and lymph node, homogenates failed to show the presence of any significant number of luminescent cells, within the detection limit of the procedure (a minimum of 10 cells/lymph node or 50–100 cells for the rest of the tested organs), indicating that cell death rather than migration was responsible for the disappearance light from the implants.

4.3. *Discussion*

The aim of the current work was the use of a model system, based on non-invasive bioluminescence imaging (BLI) of luciferase expressing cells seeded in scaffold materials, to analyze the application of RAD16-I [10, 12, 13, 40, 41, 45, 112] scaffolds and RAD16-I/biorubber composites for tissue regeneration.

Mouse embryonic fibroblasts C57Bl/6 cells, capable of growing and *in vitro* differentiating to osteogenic cells in RAD16-I hydrogels [25, 45], were used in these experiments as a model to analyze the capacity of the materials to sustain cell growth *in vivo*. In spite of their good capacity to sustain cell proliferation, the low shear stress resistance (9 Pa) of RAD16-I hydrogels could result in rapid scaffold degradation, an important restriction for their application in many tissues. To overcome this limitation we combined RAD16-I with a biorubber elastomer and the resulting composite had better shear-strain characteristics (25,000 Pa) within the range of animal tissues –Brain: 0.1–0.2 KPa, Disc Cartilage (nucleus pulposum): 0.3–0.4 KPa, Skeletal and cardiac muscle: 3–4 KPa, Joint cartilage: 100-200 KPa– and a relatively uniform (100–150 μm) pore size distribution.

In vitro, C57BL/6 cells, tagged by infection with lentiviral vectors for the expression of PLuc and EGFP (G·Luc-C57BL/6), produced 7.6 RLUs/cell stably throughout the duration of the experiments (90 days). Cells implanted in vivo were easily detectable, and analysis of BLI images, from predetermined numbers of G·Luc-C57BL/6 cells implanted in the thighs of BALB/c nu/nu mice, showed that, it was possible to detect a minimum of 1000 cells and that there was a linear correlation between the amount of light detected and the number of implanted cells, with a slope of 24.8 PHCs/cell.

The capacity of the RAD16-I hydrogels and RAD16-I/biorubber composite scaffolds to support G·Luc-C57BL/6 cell growth was first analyzed *in vitro* and then *in vivo* by BLI imaging of cells seeded in scaffolds and implanted, IM or SC, in BALB/c nu/nu mice. In vitro, G·Luc-C57BL/6 cells penetrated the RAD16-I hydrogels and grew on them forming clusters [45]. However, no cells could be observed within the biorubber material, suggesting that, although the biorubber was non-toxic for the cells, some of the scaffold characteristics, such as pore interconnectivity, material surface structure or composition limited cell penetration and colonization [113]. The implantation site conditioned cell survival *in vivo*. Thus, in SC implants, G·Luc-nC57BL/6 cells were unable to survive until the end of the experiment, regardless of whether they had been seeded or not in scaffolds, as previously reported [111]. Conversely, growth of G·Luc-C57BL/6 cells implanted IM without scaffolds suffered a pronounced crisis within the first week after implantation but then tended to reach a steady state. In general, cells survived better at IM sites whether or not they had been seeded on scaffolds, and 9 of the 16 implants retained cells after 12 weeks. It is possible that the

differential survival of cells at IM and SC sites could be related to their capacity to promote an adequate blood supply [114].

The materials tested had clearly different capacities to sustain cell growth. All the RAD16-I hydrogels were successfully colonized by the G·Luc-C57BL/6 cells *in vitro*, and when the cell seeded materials were implanted IM, in all but one case, cells survived and proliferated until the end of the experiment. However, the biorubber material could neither be colonized by cells *in vitro* nor promote proliferation *in vivo* of seeded cells when combined with RAD16-I. This was possibly the result of biorubber having too small and interconnected pores to allow tissue ingrowth, vascularization and nutrient delivery [113]. Our results show that the use of the RAD16-I as a scaffold to implant cells in live animals has a boosting effect on their proliferation and survival, as compared to cells implanted without the scaffold.

Histological analysis of mouse implants from both types of materials showed that while biorubber persisted intact for long periods of time, RAD16-I was biodegradable and could not be detected by the end of the experiment *in vivo*, likely do to hydrolysis of the peptide linkers. None of the materials appeared to elicit an immune response in normal animals as judged by the absence of infiltrating lymphocytes or inflammation. However, implanted RAD16-I/biorubber composites were found surrounded by a layer of fibrotic tissue from the host as previously reported for other materials [115, 116]. Together with the small-interconnected pores and the high stiffness (25 kPa), the observed tendency to become encapsulated could explain the failure of the material to sustain cell colonization and survival *in vivo*.

4.4. *Materials and methods*

4.4.1. Scaffolds

Two different materials were used to carry out the experiments: a 16-amino acid peptidic nanofiber scaffold (RAD16-I) [11-13, 40, 41, 45, 112] (Puramatrix®, BD, Erembodegem, Belgium) and a composite material consisting of RAD16-I with a synthetic biorubber [105], a porous structure of poly (diol citrate). The porous biorubber was produced in four steps: synthesis of a pre-polymer, preparation of a porogen mask, curing the pre-polymer and porogen extraction using an apolar solvent. The pre-polymer was obtained by mixing in a vial 1.3 g of citric acid (Sigma) (6.8 mM) and 1 g of 1,8-octanediol (Sigma) (6.8 mM). The sealed vial was then introduced in a microwave (CEM Discovery, Mathews, NC, USA) where the mix was melted at 100 ºC for 6 min, with stirring, to create a pre-polymer. The porogen structure responsible of conferring porosity to the final polymer consisted of 200 μm polystyrene beads (Goodfellow, Huntington, UK), previously sintered by heating for 2 min in a microwave oven. Following, 10 ml of pre-polymer was poured onto the previously obtained porogen mask, a 13.5 mm diameter, 50 mm high disk, and the mixture was allowed to cure at 120 ºC, under vacuum, for 4 days to cross-link the biorubber. Finally, the polystyrene mask was extracted using toluene (Sigma) and cut to the desired final size. The microstructure of the obtained biorubber was characterized using a Scanning Electron Microscopy (SEM). First, the biorubber was frozen in liquid nitrogen and crushed without deforming the structure. The biorubber was gold coated and imaged using a JEOL scanning electron microscope (JSM-5310).

4.4.2. Material characterization

Rheometry. RAD16-I hydrogel, prepared as explained in Section 3.4.3, was analyzed using a standard rotational shear stress vs. shear rate experiment, in an AR 550 Rheometer (TA Instruments, West Sussex, UK). The conditions used were the following: ramp of shear stress from 0 to 10 Pa in 10 min and constant temperature at 35 ºC.

Mechanical properties. To analyze the biorubber and the RAD16-I/biorubber composite (prepared as explained in Section 3.4.3), the materials were characterized using a Dynamical Mechanical analyzer DMAQ800 (TA Instruments). A compression clamp and a constant temperature of 35 ºC were used in all experiments. Two different sets of experiments were carried out using the instrument methods of: I) Strain rate method: a strain ramp from 0 to −35% (compressive behaviour) was applied, and the compressive stress was recorded. II) Creep method: a constant compressive force of 0.05 N was applied to the samples during 15 min and the deformation vs. time was recorded.

4.4.3. Lentivirus production and cell labeling

The lentiviral vector containing the enhanced green fluorescent protein (EGFP) gene under the control of the simian virus SV40 promoter and the *P. pyrallis* luciferase (Luc) gene (Promega Corporation, Madison, WI) under the control of the cytomegalovirus promoter,was constructed by cloning the cassette between the ClaI and BamHI sites of the lentiviral vector Plox/Twgfg provided by Dr. D. Trono (Ecole Polytechnique Fédérale de Lausanne, Lausanne, Switzerland).

Human embryonic kidney cells 293T, obtained from the ATCC (Rockville, Maryland, USA), were used for viral production as previously described [109]. Viral particles were resuspended with PBS 1X and kept at -80 ºC. Viral titration was performed using the HIV-1 p24 antigen EiA (Beckman Coulter) 96 test kit.

Mouse Embryonic Fibroblasts (C57BL/6 cell line, ATCC) were cultured in Dulbecco's Modified Eagle Media-high glucose (DMEM-Hg) (Sigma, Steinheim, Germany) supplemented with 10% heat-inactivated fetal bovine serum (FBS) (Sigma), 50 units/ml penicillin/streptomycin (Sigma) and 4 mM L-glutamine (Sigma). At passage 2 cells were plated at 6500 cells/cm2 in 12-well plates. The following day an aliquot of viral particles (MOI 1/421 infectious viral particles/cell) was diluted in 1 ml of growth medium containing 10 μg/ml polybrene (Sigma) and added to the cells. After 48 h in culture, virus-containing medium was replaced by fresh medium and cells were allowed to grow. The highest 30% eGFP expressing cells (G·Luc-C57BL/6) was selected by FACS, expanded and used for seeding the scaffolds.

4.4.4. Luciferase assays and DNA quantification

An aliquot of G·Luc-C57BL/6 cells was maintained in culture to monitor luciferase expression during the course of the experiment. Every 15 days cells were trypsinized, counted and an aliquot containing $2 \cdot 10^5$ cells was suspended in reporter lysis buffer (RLB) 1X (Promega) and stored frozen at -80 ºC (cell lysate). At the end of the experiment the collected samples were used to determine luciferase activity and DNA concentration as detailed previously [109].

4.4.5. Cell seeding

G·Luc-C57BL/6 cells were trypsinized, suspended in a solution of sucrose 10% in deionized water (pH 6.1) (Sigma) and mixed with RAD16-I peptide (BD) to attain a final concentration of $2 \cdot 10^6$ cells/ml in 0.25% RAD16-I peptide solution. Plastic inserts (Millipore, Billerica, MA, USA) were placed in 12-well tissue culture plates leaving a space between the well and the insert. Biorubber pieces were placed in the plastic inserts to create the RAD16-I/biorubber composite. Then, 100 μl of the cell suspension in RAD16-I peptide was pipetted into the insert (with or without biorubber) and 250 μl of growth media were added to the space between each insert and well. The material was allowed to gel at 37 ºC for 5 min and 400 μl of growth media were layered onto the hydrogel. Changing 2/3 of the media after 30, 60 and 120 min

post gelling equilibrated the construct pH. RAD16-I hydrogels and RAD16-I/biorubber scaffolds were also prepared without cells to analyze the materials biocompatibility. However, as RAD16-I is transparent, to facilitate histological detection of *in vivo* implants, a mixture of RAD16-I and biotinylated RAD16-I (RAD16-Ib) (3:7), respectively, was used. In vitro cultivation of RAD16-I and RAD16-I/biorubber seeded scaffolds was performed at 37 ºC with 5% CO2 and medium was changed every 2 days. Scaffolds were cultured in vitro during 15 days before being implanted. At this cultivation stage the stiffness of these constructs could match the tissue implanted and allow cells to proliferate due to the new vascular-rich environment, the muscle.

4.4.6. Mice

Six-week-old BALB/cAnNCrl mice were used to test scaffold biocompatibility and six-week-old BALB/c homozygous nude (nu/nu) mice were used to monitor the in vivo behavior of G·Luc-C57BL/6 cells injected with or without scaffolds. All animals were purchased from Charles-River (Wilmington, MA); BALB/c nu/nu mice were maintained in a specific pathogen-free environment. Animal procedures were performed with the approval of the animal care committee of the Cardiovascular Research Centre and the Government of Catalonia.

4.4.7. Scaffold implantation

Animals were anesthetized by intraperitoneal injection of 100 mg/kg ketamine (Merial, Duluth, GA) and 3.3 mg/kg xilacine (Henry Schein, Melville, NY), and additionally received a subcutaneous analgesic injection of 0.05 mg/kg buprenorphine (Schering-Plough, Kenilworth, NJ). The inoculation place was shaved (BALB/c mice) and cleaned with povidone-iodine (Braun, Melsungen, Germany). Four implantations were performed in each animal: two subcutaneous (SC) on the back and one intramuscular (IM) in each thigh. Animals received RAD16-Ib hydrogel (BALB/c) or RAD16-I hydrogel + G·Luc-C57BL/6 (BALB/c nu/nu) on the right side and RAD16 Ib/biorubber composite (BALB/c) or RAD16-I/biorubber + G·Luc-C57BL/6 composite (BALB/c nu/nu) on the left side. For each implantation, an incision was performed on the skin and a small pocket was formed subcutaneously (SC implants) or in the thigh muscle (IM implants). Then, 30 μl of the gelled material were implanted using a syringe fitted with a bevel ended pipette tip. The incision was closed using absorbable sutures. The control group for the in vivo evaluation of G·Luc-C57BL/6 cells, comprised three mice (BALB/c nu/nu) receiving each one four injections (two SC and two IM, in each thigh) of $1.5 \cdot 10^5$ G·Luc-C57BL/6 cells suspended in medium without FBS.

4.4.8. Bioluminescence imaging

In vivo optical imaging of implanted nude mice was performed as described previously [109]. Mice were anesthetized with ketamine/xilacine and immobilized. Following the inoculation of 50 μl of D-luciferin (100 mg/kg, Promega) *in situ* (SC or IM) the mice were placed in the detection chamber of a high-efficiency ORCA-2BT Imaging system (Hamamatsu Photonics, Hamamatsu City, Japan) provided with a C4742-98-LWG-MOD camera and a 512 x 512 pixel, charge couple device (CCD) cooled at -80 ºC at a distance of 247 mm from the camera objective (HFP-Schneider Xenon 0.95/25 mm). Two images were acquired of each mouse, one using a white light source inside the chamber to register the animal position and a second one, in total darkness, during a 5 min period to acquire photons (PHCs) from the light emitting cells. Images were taken at 0, 7, 15, 30, 45 and 90 days post-implantation. Quantification and analysis of recorded PHCs were done using the Wasabi image analysis software (Hamamatsu Photonics).

To establish the cell detection sensitivity *in vivo*, a standard curve was generated by imaging predetermined numbers of cells (10^3, $5{\cdot}10^3$, 10^4, $5{\cdot}10^4$, 10^5, $2.5{\cdot}10^5$) grafted IM in BALB/c nu/nu mice.

4.4.9. Cell migration

To determine if cells from the implants had migrated to other organs, at the end of the 3-month *in vivo* implantation period, one control (no scaffold) and two scaffold implanted mice (the ones producing most light at the implantation site) were sacrificed, dissected and target organs (brain, liver, spleen, lungs, ribs and lymph nodes) harvested. Luciferase activity, indicative of the presence of cells from the implants, was determined on tissue homogenates using a sensitive luminometric procedure as described [117].

4.4.10. Histology

In vitro cultured gels were washed, fixed with 4% paraformaldehyde (PFA) for 2 h and embedded in paraffin. 5 μm thick sections of the embedded scaffolds were stained with hematoxylin-eosin. To detect RAD16-Ib, sections were deparaffinized, rehydrated and washed in PBS 1X. Then the sections were incubated with the ABC reagent (Dako, Glostrop, Denmark) for 30 min in darkness and processed for diaminobenzidine (DAB) staining (Roche, Basel, Switzerland) following the manufacturer instructions. Sections were also counterstained with hematoxylin-eosin (Sigma) as previously described [118].

After the 90 days *in vivo* period, animals were sacrificed by cervical dislocation and IM and SC implanted samples were harvested when present. Samples were washed with PBS 1X and fixed with 4% PFA (Sigma) for 24 h at 4 ºC. IM samples were then placed over an ion-exchange resin (Amberlite IR-120(plus) ion-exchange resin, sodium form, Sigma) and

decalcified with formic acid 10% for 24 h at room temperature. Then all samples were embedded in paraffin and serially sectioned (10–14 μm thick).

BALB/c sections were stained with hematoxylin–eosin or with the ABC staining. BALB/c nu/nu sections were stained with hematoxylin–eosin or with the Masson-trichrome method [119], which reduces fluorescent background of the muscular tissue, improving the detection of the implanted G·Luc-C57BL/6 cells.

4.4.11. Statistical analysis

Statistical analysis was performed using the StatView version 5.0. A two-way ANOVA test was performed to compare proliferation of injected G·Luc-C57BL/6 cells, G·Luc-C57BL/6 cells seeded in RAD16-I hydrogel and G·Luc-C57BL/6 cells seeded in RAD16-I/biorubber composite. Statistical significance was considered when $p < 0.05$.

5. Rational design and development of biomimetic nano-structured hybrid materials for bone and cartilage regeneration

5.1. *Introduction*

Tissue engineering is a scientific discipline that brings together biology, materials science and even electronics to produce artificial constructs for the replacement of dysfunctional organs [8]. In the previous chapters, we have presented the biological *in vitro* and *in vivo* approaches we adopted to generate a new paradigm for the repair of bone-like and cartilaginous tissues. In this final chapter, we will discuss the development of biomimetic materials that help in the production of tissue-engineered grafts.

There has been extensive work in the field of cartilage and bone regeneration for they are two of the least complicated tissues in the body. Pubmed searches for “cartilage tissue engineering” and “bone tissue engineering” have rendered 549 and 1288 entries respectively only during the last year (Pubmed, NCBI, 03/11/09). Moreover, bone marrow hematopoietic stem cell transplants have been one of the first widely used cell therapies applied ever [120] and there are currently several cell-based therapies in use or in clinical trials for the regeneration of bone and cartilage conditions [15, 121-124]. Bone and cartilage replacement materials have also been long used in medicine [125-127]. However, a problem that is still not resolved in skeletal tissue engineering is the joint between articular cartilage and bone. Natural unions of cartilage and bone are a gradual change from cartilage to bone ECM. This gradual transition has not been yet reproduced artificially and it was our wish to contribute to the development of materials to match this unmet need.

Specifically, we have developed surface modified hydroxyapatite (HA) microparticles that we expect to use as charges in cartilage-like engineered tissues. These coated HA charges will enable to control the calcification of the engineered grafts, as happens in the natural bone-to-cartilage joint. More interestingly, the coating will allow controlling the physical and biological properties of the charges (dispersibility, solubility, growth factor attachment…). Our group has already developed methods to coat particles using plasma polymerization techniques [27, 28].

Plasma-initiated polymerization processes are mostly driven to the formation of thin films. In this work we have used two different plasma-enhanced techniques for the coating of surfaces: the Plasma Enhanced Chemical Vapor Deposition (PECVD) and the Plasma Grafting Polymerization. PECVD consists on the deposition of thin films from a vapor of monomer that is activated as plasma. This activated monomer binds to the surface of any material and polymerizes. In the plasma grafting process, the sample is first ionized and ion-sputtered with high-density plasma and the resultant activated surface is submitted to contact with a monomer. The radicals and ions present on the sample act as initiators for the polymerization of the monomer.

Here we have coated HA microparticles by PECVD, but as there are concerns that the chemical binding between activated organic monomers and ceramics is not strong enough to

resist organic solvent treatments we decided to try a method to have a tighter attachment between HA and the deposited film. An organosilane coating between HA and the polymer could help in this purpose because silane compounds have good chemical affinity for both inorganic and organic materials. In this particular case, organosilanes have high affinity for HA, thanks to their silane group, and a carbon chain that will easily react with activated organic monomers to form attached polymer chains [128]. To increase the reactivity between the silane and the activated organic monomer, the silane chosen was (3-aminopropyl)-trimethoxysilane (AMMO), a compound that has a reactive amine in its side chain.

Apart from the coating of particles to produce high quality biocompatible charges, we were also interested in producing versatile platforms to use in combinatorial biological assays. For this purpose, chemically reactive 96-well plates of modified polystyrene would be very useful. Thus we proposed to coat 96-well plates with the chemically reactive group pentafluorophenyl methacrylate (PFM) to render a platform prepared to link to any biological compound including proteins, nucleic acids… The plasma-initiated polymerization of polymers has long been used in surface coating [129-134] and more concretely deposition of poly(pentafluorophenyl methacrylate) has also been developed in the recent years as a reliable method of producing chemically active surfaces [135-138]. In this work, though, we will not deposit PFM by PECVD as it is done in the literature, but we will use Plasma Grafting instead.

The pentafluorophenyl esther in the PFM is a reactive group that can bind to virtually any protein or alcohol [135-137], thus a plate coated with such a film would allow to perform combinatorial assays with compounds having amino or alcohol groups such as sugars or proteins. The resulting platform could be of great use in determining cell response to a high diversity of biochemical stimuli, which usually consist on small peptides, sugars or combinations of both.

The optimal set-up for the production of modified plates was established using the Doehlert second order multi-factorial experimental design. The Doehlert matrixes as well as other second order surface response designs are frequently used to adjust formulations in the industry [139-142] or reactors' set-ups [143]. In addition, this design permits study of the factors at a different number of levels (3, 5 and 7), thus giving to the researcher the possibility to study some factors in greater.

In summary, we intend to continue with the studies of Garreta et al. [27, 28] and produce coated HA for use in regenerative medicine. We will use synthetic as well as commercial HA and compare their performance by themselves and after being coated with polyacrylic acid, a hydrophilic polymer. We will also work on the production of PFM modified 96-well plate for use in combinatorial biochemistry and biology.

5.2. *Results*

5.2.1. Synthetic tailor-made HA has different properties compared to the commercial one

There has been extensive work in our research group to support the significant difference between the behaviors of synthetic and commercial HAs [26-29]. In this thesis we present another experimental evidence to support the different physical and chemical properties of these two types of HA.

We produced tailor-made HA by a sol-gel synthetic method previously developed in the group following literature's instructions [144]. We compared commercial HA (Captal®, Biotal Plasma Limited Inc.) with our synthetic HA and XRD spectra from both samples pointed out that Captal® is more crystalline than our tailor-made HA (**Figure 22**). That Captal® is more crystalline than synthetic HA was also described before [29], comparing Ca^{2+} exchange rates of the different HA in simulated body fluid. Captal® had a much lower Ca^{2+} exchange than synthetic HA, which indicates that Captal® has a higher crystalline structure. In fact, these studies showed that tailor-made HA had a higher rate of biocompatibilization than Captal® not only in terms of calcium exchange with Simulated Body Fluid (SBF) but also in the formation of complex HAs with carbonates and nitrates on the surface of the particles, rendering forms of HA extraordinary similar to natural bone apatite [29].

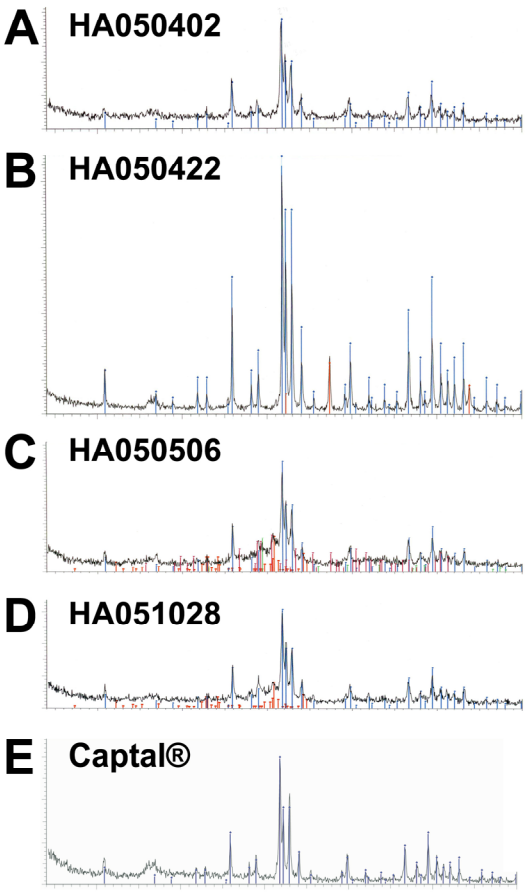

Figure 22: XRD spectra of tailor-made hydroxyapatites and commercial Captal®
(**A-D**) XRD spectra of 4 different synthesized hydroxyapatites. **A** and **B** are very pure HAs but with different degree of crystallinity, being **B** the highest of all. **C** and **D** represent less pure HA, that usually have tricalcium phosphate, calcium nitrates and calcium carbonates as principal impurities. (**E**) XRD spectrum of Captal® shows that it is a pure and crystalline HA. The height of the XRD peaks indicates that Captal® is more crystalline that all tailor-made HAs except for **B**, that was obtained at higher temperature compared to the other tailor-made HAs (See materials and methods).